# A review of electrodynamic tethers for science applications

**J R Sanmartin**

Universidad Politécnica de Madrid, Pza. C. Cisneros 3, Madrid 28040, Spain

E-mail: juanr.sanmartin@upm.es

**Abstract**

A bare electrodynamic tether (EDT) is a conductive thin wire or tape tens of kilometres long, which is kept taut in space by gravity gradient or spinning, and is left bare of insulation to collect (and carry) current as a cylindrical Langmuir probe in an ambient magnetized plasma. An EDT is a probe in mesothermal flow at highly positive (or negative) bias, with a large or extremely large 2D sheath, which may show effects from the magnetic self-field of its current and have electrons adiabatically trapped in its ram front. Beyond technical applications ranging from propellantless propulsion to power generation in orbit, EDTs allow broad scientific uses such as generating electron beams and artificial auroras, exciting Alfven waves and whistlers, modifying the radiation belts and exploring interplanetary space and the Jovian magnetosphere. Asymptotic analysis, numerical simulations, ground and space tests and past and planned missions on EDTs are briefly reviewed.

## 1. Introduction: electrodynamic tether (EDT) basics

A space tether is a kilometer long wire connecting two satellites. Assuming that the tether remains vertical in a circular orbit, and its mass is small compared with end masses $m_1$ and $m_2$ at the bottom and the top, the common rotation velocity $\omega_{\rm orb}$, in the absence of any other force, is determined by the overall balance of gravitational and centrifugal forces in the orbiting frame,

$$\omega_{\rm orb}^2\,(m_2 r_2 + m_1 r_1) = GM_{\rm E}(m_1 r_1^{-2} + m_2 r_2^{-2}), \qquad (1)$$

where $M_{\rm E}$ is the Earth's mass. There is a radius $r_0$ where gravitational and centrifugal forces are equal, $r_1 < (GM_{\rm E}/\omega_{\rm orb}^2)^{1/3} \equiv r_0 < r_2$. The centrifugal force is greater for the upper mass $m_2$, which is thus subject to a net force away from the Earth. The opposite holds for the lower mass. This results in tether tension making the vertical orientation stable [1].

There is a *gravity gradient* force per unit mass at points away from $r_0$,

$$3\omega_{\rm orb}^2(r - r_0) \qquad (\text{for } r_2 - r_1 \equiv L \ll r_1). \qquad (2)$$

If the tether is conductive and carries a current as a result of interaction with the magnetized ionosphere, it will also experience a magnetic force. In addition, there is some bowing, and a Lorentz torque that may be balanced by a gravity-gradient torque at a tether tilt. All past missions involving tethers either used low Earth orbit (LEO) or were suborbital flights [2].

A Lorentz transformation in the non-relativistic limit relates electric fields in frames moving with spacecraft and local co-rotating plasma,

$$\bar{E}(\text{tether frame}) - \bar{E}(\text{plasma frame}) = (\bar{v}_{\rm orb} - \bar{v}_{\rm pl}) \wedge \bar{B} \equiv \bar{E}_{\rm m}. \qquad (3)$$

In the highly conductive ambient plasma outside the tether (meters away, typically) the electric field is negligible in the local plasma frame. There is then, in the tether frame, an outside ('motional') field $\boldsymbol{E}_{\rm m}$ that drives a current $\boldsymbol{I}$ inside the tether with $\boldsymbol{I} \cdot \boldsymbol{E}_{\rm m} > 0$ in the case of a passive tether system. The Lorentz force on an insulated tether of length $L$ carrying a uniform current reads $L\boldsymbol{I} \wedge \boldsymbol{B}_0$. Since Newton's 3rd law applies to magnetic forces between steady-current systems, a net power loss is seen to occur in the tether–plasma interaction,

$$L\bar{I} \wedge \bar{B}_0 \cdot \bar{v}_{\rm orb} + (-L\bar{I} \wedge \bar{B}_0) \cdot \bar{v}_{\rm pl} \equiv -\bar{I} \cdot \bar{E}_{\rm m} L < 0, \qquad (4)$$

which is (Lorentz) power naturally feeding the tether electric circuit [3].

The Lorentz force is a drag in LEO for both prograde and retrograde circular equatorial orbits, with $\boldsymbol{v}_{\rm orb}$ and $\boldsymbol{v}_{\rm orb} - \boldsymbol{v}_{\rm pl}$ in the same direction. For a vertical tether in prograde

LEO, and a non-tilted, centered magnetic dipole model ($\boldsymbol{B}_0$ northward, $\boldsymbol{E}_m$ upward), a typical 'motional' field is $E_m = v_{orb}B_0 \sim 7.5\,\mathrm{km\,s^{-1}} \times 0.2\,\mathrm{G} = 150\,\mathrm{V\,km^{-1}}$, westward Lorentz drag and drag power reading $F_M = LIB_0$, $W_M = F_M v_{orb} = IE_m L$. Although issues of scientific interest will be considered here, the fundamental area of application of tethers is propellantless transportation [4]. The magnetic force on a tether requires no ejection of propellant, as opposite rockets or electrical thrusters, and no power supply. Hollow cathodes used for cathodic contact do eject (xenon) expellants along with electrons but at extremely low rate; also, required bias is just tens of volts, leading to negligible contact impedance [5].

On the other hand, tether performance is ambient dependent. The bottleneck is the anodic contact: how to efficiently collect electrons from the rarefied ionosphere. The TSS-1 and TSS-1R tethers carried a conductive sphere of radius $R = 0.8\,\mathrm{m}$ acting as passive collector. Space charge keeps the electric field to a sheath around the sphere (ionospheric Debye length $\lambda_D$ is a fraction of a centimeter) and the geomagnetic field guides electrons along field lines (electron gyroradius $l_e$ is a few centimeters); this strongly limits the current to a spherical collector [6]. The PMG tether used plasma contactors for both electron ejection *and* collection, which proved poor, however [7].

## 2. The cylindrical probe at highly positive bias

In 1991 it was proposed that [8], instead of using a large end-collector, a tether be left bare of insulation, acting as a giant cylindrical Langmuir probe in the orbital-motion-limited (OML) regime [9]. Collection is efficient because the cross-section is small, while the collecting area is large because the anodic segment may be multikilometers long. Magnetic force and power now involve the length-averaged current $I_{av}$, but a length-to-radius ratio $\sim 10^6$ makes each point collect current as in a probe uniformly polarized at a local bias $\Delta V$ [8].

The electron current to a cylindrical or spherical probe at rest in a collisionless, unmagnetized, Maxwellian plasma of density $N_0$ and temperatures $T_e$ and $T_i$ may be written as $I = I_{th} \times$ a function of $e\Delta V/kT_e$, $R/\lambda_D$, $T_i/T_e$, with $I_{th}$ the random current. Determining electron trajectories to find $I$ requires solving Poisson's equation for the potential $\Phi(r)$, with $\Phi(R) = \Delta V > 0$ and $\Phi(\infty) = 0$. This requires solving for the density $N_e$ of attracted electrons (the density of repelled ions follows the Boltzmann law except where fully negligible anyway). Since the distribution function of electrons (originating at the ambient plasma) is conserved along trajectories, its value at given $\vec{r}$, $\vec{v}$ will be the undisturbed Maxwellian $f_M$ if their trajectory connects back to infinity, and zero otherwise.

For a cylinder, the density $N_e(r)$ will be an integral of $f_M$ over $v_z$ (along the cylinder) and over all energies $E \equiv \frac{1}{2}m_e(v_r^2 + v_\theta^2) - e\Phi(r) > 0$, once for radial velocity $v_r < 0$ and again for $v_r > 0$, and a $r$, $E$-dependent range of angular momentum $J \equiv m_e r v_\theta$:

(i) For a $v_r < 0$, $E$-electron at $r$ the range of integration is
$$0 < J < J_r^*(E) \equiv \text{minimum}[J_{r'}(E);\ r \leqslant r' < \infty],$$
$$J_r^2(E) \equiv 2m_e r^2[E + e\Phi(r)].$$

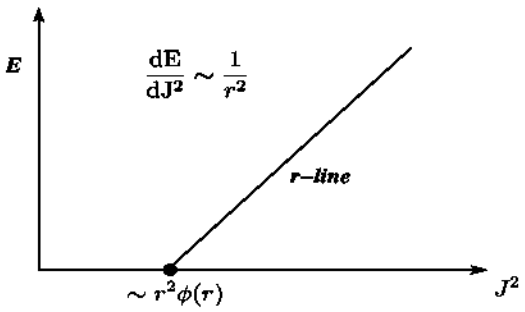


**Figure 1.** A $J^2 = 2m_e r^2[E + e\Phi(r)]$ line.

Condition $v_{r'}^2 \geqslant 0$ reads $J \leqslant J_r(E)$ but $v_{r'}^2 > 0$ is required throughout the range $r \leqslant r' < \infty$.

(ii) For a $v_r > 0$, $E$-electron, the range of integration is $J_R^*(E) < J < J_r^*(E)$, electrons in the range $0 < J < J_R^*(E)$ having disappeared at the probe.

Collected current $I$ and density $N_e$ as a functional of $\Phi(r)$ are then

$$\frac{I}{I_{th}} = \int_0^\infty \frac{dE}{kT_e}\exp\left(\frac{-E}{kT_e}\right)\sqrt{\frac{2\left[J_R^*(E)\right]^2}{\pi m_e R^2 kT_e}}, \tag{5}$$

$$\frac{N_e}{N_0} = \int_0^\infty \frac{dE}{\pi kT_e}\exp\left(\frac{-E}{kT_e}\right)\left[2\sin^{-1}\frac{J_r^*(E)}{J_r(E)} - \sin^{-1}\frac{J_R^*(E)}{J_r(E)}\right]. \tag{6}$$

With $J_R^*(E) \leqslant J_R(E)$, maximum current occurs if the equality holds for $0 < E < \infty$, which is the OML regime, the ratio $I_{OML}/I_{th}$ depending only on $e\Delta V/kT_e$ and reading at high bias,

$$I_{OML} \approx I_{th} \times \sqrt{4e\Delta V/\pi kT_e} = 2RLeN_0\sqrt{2e\Delta V/m_e}. \tag{7}$$

The $\Phi(r)$-dependent structure of the $r$-family of straight lines $J^2 = J_r^2(E)$ in the $J^2$–$E$ plane determines the functions $J_r^*(E)$ and $J_R^*(E)$, which in turn determine $N_e$ for use in Poisson's equation. Since the slope $dE/dJ^2 = 1/2m_e r^2$ varies monotonically with $r$, it suffices to have $J_r^*(0) = J_r(0)$ for $J_r^*(E) = J_r(E)$ to hold for all positive $E$, at any particular $r$ (figure 1), but $J_r^2(0)$ varies as $r^2\Phi(r)$ which proves non-monotonic; this results in a complex $r$-family structure. The OML condition, however, requires the potential to just satisfy $J_R^*(0) = J_R(0)$, i.e. $r^2\Phi(r) > R^2\Delta V$ throughout the range $R < r < \infty$. Faraway 2D quasineutrality, $N_e \approx N_i$, shows a behavior $\Phi r^2 \sim r$. Moving toward the probe, $r^2\Phi(r)$ decreases to a minimum (lying far from the probe for high bias and $R \sim \lambda_D$); the quasineutral solution remains valid up to a sheath boundary, where $-d\Phi/dr$ diverges. Within the sheath $r^2\Phi(r)$ reaches a large maximum (at minimum $N_e$) before again dropping to $R^2\Delta V$ at the probe (figure 2) [10].

The OML current law for a cylinder is robust; the ratio $I_{OML}/I_{th}$ is independent of the ion distribution function, of the electron distribution if isotropic and of $R/\lambda_D$ and $T_i/T_e$ values over a large parameter domain. If $R$ exceeds some radius $R_{max}$ the ratio $I/I_{OML}$ drops below 1 and decreases with increasing $R/R_{max}$. The $r^2\Phi(r)$ minimum then lies below $R^2\Delta V$, trajectories that hit the probe within a range of glancing angles being unpopulated; they come from other

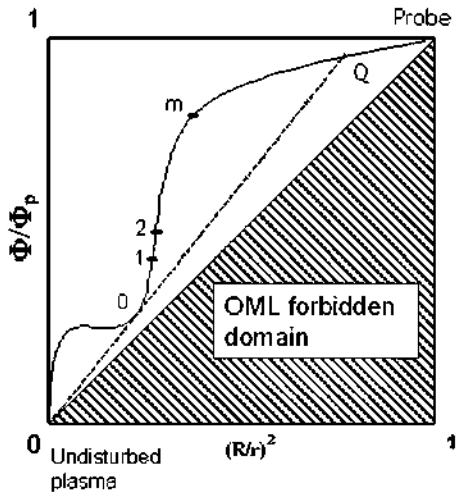


**Figure 2.** Potential versus $1/r^2$ in the OML regime, from [11], where $\Phi_p$ is the bias $\Delta V$.

probe points after turning back in the far field [10]. Recent asymptotic analyses [11] fully agree on $R_{max}$, current beyond $R_{max}$, and $\Phi$ and $N_e$ profiles, with results from steady Vlasov calculations and particle-in-cell simulations [12]. (The OML current to a sphere considerably exceeds the 2D current for equal $I_{th}$ and bias, but is never reached; faraway behavior is now $\Phi r^2 = \text{const} < R^2\Delta V$, typically rising above $R^2\Delta V$ very close to the probe.)

## 3. Adiabatic trapping and other bare-tether issues

For a passive tether system, current is limited by the short circuit value, $\sigma_c E_m A_t$ ($A_t$ being cross-section area), arising from the tether resistance $Z_t \equiv L/\sigma_c A_t$. Tether performance may depend on additional design parameters in the overall electric circuit: the load impedance in a power generation mode and both electric power supplied and length of insulated segment next to the top in a thrusting mode (a thrusting tether would be inefficient if fully bare). The overall system is also characterized by a dimensional parameter $\rho/\sigma_c E_m^2 \approx 3.43\,\text{kg kW}^{-1}$ for Al and $E_m = 150\,\text{V km}^{-1}$, which corresponds to the inverse specific power of power systems.

Ohmic effects are gauged by comparing the short circuit current with an average of the OML current in (7) for some length $L^*$ and bias $E_m L^*$. This determines $L^*$ [8],

$$L^* \propto E_m^{1/3} (\sigma_c A_t / p N_0)^{2/3}. \tag{8}$$

Collection performance is optimum for $L \gg L^*$, when current is maximum for a given tether mass and the bare-tether contact impedance is negligible. This suggests moving away from round wires. The OML law is valid for any convex cross-section shape [9], with OML current-density uniform over the probe surface; it suffices to write $p/\pi$ instead of $2R$ in equation (7).

As regards non-OML results, there is an equivalent radius $R_{eq} \neq p/2\pi$ for any cross-section. Because of the high bias, Laplace's equation holds in a large probe vicinity, reaching where the electric field is about radial; this allows determining $R_{eq}$ as a classical problem in the capacitance per unit length of coaxial lines. For a thin tape, $R_{eq}$ is $p/8$. A tape collects the same OML current as a round wire of equal perimeter, while being much lighter, the optimal tether thus presenting three disparate dimensions, $L \gg$ tape width $w \gg$ thickness $\delta$. This reflects on length $L^*$ varying as $R^{2/3}$ for round wires and as $\delta^{2/3}$ for tapes [13].

The resilience of the OML law further shows in its being reasonably applicable to non-convex cross-sections, for which it breaks independently of size due to the behavior of the potential near the probe; the law may still be used if $p$ is replaced by the perimeter of the minimum-perimeter envelope of the cross-section [13]. All the above results apply, however, to unmagnetized plasmas at rest. Geomagnetic effects might in principle break the 2D-OML law because of 3D effects. There is, however, an upper (Parker-Murphy) bound to current to a cylinder in a magnetized plasma, reading at high bias [14]

$$I_{PM} \approx I_{OML}\sqrt{2/\pi} \times l_e/R. \tag{9}$$

The geomagnetic field is thus expected to hardly affect the current for $R \ll l_e$.

The field due to the tether own current might reduce current collection. Strong reduction would occur roughly at tether points where some average radius $r^*$ of a magnetic separatrix modifying field topology in the cross-section plane exceeds the sheath radius $r_{sh}$ [15],

$$r_{sh} < r^* \equiv I/2\pi\varepsilon_0 c^2 B_0. \tag{10}$$

Self-field effects, however, are typically negligible for thin tapes because ohmic effects severely limit current and separatrix radius. They are also negligible for round tethers at the Van Allen Belts, at Jupiter, and in interplanetary space, where the plasma density is very low.

As regards $v_{orb}$ effects, the 2D-OML law might hold in principle because the plasma flow in LEO barely breaks ambient electron isotropy. However, the mesothermal character of that flow raises a paradox for the high-bias tethers. With the ambient electron population (nearly) isotropic, a fundamental result [9] shows $N_e < N_0$ in any 2D potential field $\Phi(r,\theta)$. On the other hand, the high bias would ram back the 5 eV hypersonic ions, yielding $N_i(r,\theta) > N_0$ and thus breaking quasineutrality over front distances much larger than $\lambda_D$.

The way out of this quandary seems to hinge on $E < 0$ electrons trapped in bound trajectories not accounted for in [9]. The key process is collisionless (adiabatic) trapping. As troughs in electron potential energy develop when quasineutrality is first broken, electrons are trapped in fast bound orbits slowly changing in an unsteady potential controlled by ion motion, finally leading to steady quasineutrality [16].

Laboratory tests involving the combined plasma-flow and magnetic effects have proved inconclusive. Bare-tether current collection by the long lattice of tensioning rods for each mast in the International Space Station solar array did explain, however, current balance in the Station south of Australia

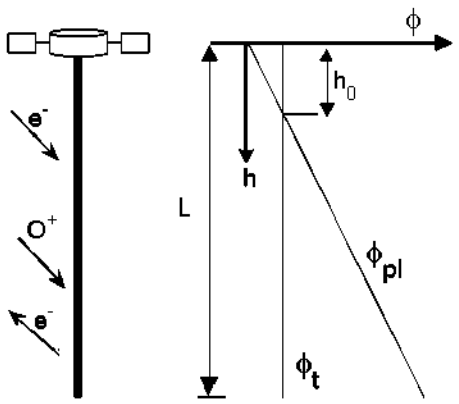


**Figure 3.** Electrically floating tether.

in early 2001. Also, bare-tether collection will be tested in 2010 by a dedicated sounding-rocket mission (S-520-25) of the Japanese Space Agency [17]. Note that, to ensure 2D, cylindrical conditions in testing high-bias OML collection, length $L$ must be much larger than sheath radius, not just much larger than $R$,

$$r_{sh}/\lambda_{De} \approx 2\sqrt{e\Delta V/kT_e} \gg 1, \qquad \text{for } R \sim R_{max} \sim \lambda_D. \tag{11}$$

## 4. Determining *E*-layer neutrals density profiles

If the cathodic contactor is switched off, a tether *floats* electrically, i.e. current vanishes at both ends. Because of the large ion-to-electron mass ratio, the floating tether is biased negative except over a small fraction of its length at the top, $h_0/L \sim (m_e/m_i)^{1/3} \approx 0.03$ (figure 3). The low ion current makes for negligible ohmic effects, bias increasing linearly with distance $h$ from the top at the $E_m$ rate. Ambient ions impacting the tape both leave as neutrals and liberate additional secondary electrons, which race down the magnetic field and excite neutral molecules in the E-layer, resulting in auroral emissions [18].

The electron beam from a tether is free from effects marring the 'standard' beams introduced in 1969 for producing artificial auroras. Tether emission takes place far from any instrument, and has no effect on S/C potential. Beam density and flux are low, thus avoiding nonlinear plasma-interaction problems that arise with standard beams, which require high flux to make thin-beam ground observation possible [19]. Beam is about twice the electron gyroradius [$\propto$ (energy)$^{1/2}$] thick, flux being less than $10^{-3}$ times the ambient plasma flux at emission, and the beam-to-ambient electron density ratio being less than $10^{-5}$,

$$\Phi_\infty(h) \approx N_0\Omega_e w\sqrt{\frac{m_e}{m_i}}\frac{\gamma(eE_m h)}{2\pi\cos(\text{dip})}, \tag{12}$$

$$\frac{N_b}{N_0} \approx \sqrt{\frac{m_e}{m_i}}\frac{w}{l_e}\frac{\gamma(eE_m h)}{4\sqrt{2}\cos(\text{dip})}\sqrt{\frac{kT}{eE_m h}}, \tag{13}$$

where $\gamma$ is the energy-dependent secondary yield, $\Omega_e$ the electron gyrofrequency, and dip the magnetic dip angle.

Each point in the tether emits monoenergetic secondary electrons with a definite pitch-angle distribution, and energy and flux increasing with distance $h$. As beam electrons move in helical paths down the magnetic lines, they find a density of neutral molecules increasing with decreasing altitude $z$. Beam electrons lose energy in inelastic ionization and excitation collisions, followed by photon emission; they are also scattered in elastic collisions with air molecules, which both affect pitch distribution and beam flux through diffusion across magnetic lines. The beam dwell-time at any particular point does permit excited states with prompt emission through *allowed* transitions (lifetimes $\sim 10^{-7}$ s) to reach a steady state, emission rates then being proportional to excitation rates. Since cross-sections have similar energy dependence for all collisional interactions, there exist simple approximate relations between emission and ionization rates for prominent spectral bands and lines.

The low-flux, thin beam exhibits brightness for ground observation as low as 1 *Rayleigh*, light sources in the night sky masking such signals. On the other hand, brightness is much greater for observation from the spacecraft, over a hundred *Rayleigh* for prominent bands and lines, say 427.8 or 391.4 nm for $N_2$, and 777.4 and 844.6 for $O$ and $O_2$, allowing continuous measurements (impractical for standard-beam cross-sections). They involve 'column'-integrated emission rates along straight lines extending over the ionization region and determining a relation $z$ ($h$, $\psi$); brightness, at each small angle $\psi$ from the magnetic field, mix $z/h$ effects.

As a result, the narrow emission footprint of the beam, which is tens of kilometers long and covers a line-of-sight range from the $f$-layer density maximum of about 6°, shows a peak in brightness. Tomographic inversion to determine vertical profiles of densities involves density values at a number of altitudes equal to the number of pixels along one side of an imaging camera, each pixel corresponding to a line of sight. Inversion requires a regularization technique in an iterative solution scheme involving a linearized kernel matrix. A direct approximation to the actual density profile used as good initial guess to start the iteration, which would not converge otherwise, is first obtained by fitting parameters in a model and using a Direction Set (Powell) technique [18].

## 5. Tether wave radiation

A tether carrying a steady current in the orbital frame ($\omega = \boldsymbol{v}_{rel}\cdot\boldsymbol{k}$, $\boldsymbol{k} \equiv$ wave vector), radiates waves with refraction index $n \equiv ck/\omega \gg 1$, just allowing slow extraordinary (SE), fast magnetosonic (FM) and Alfven (A) wave emission into the ionospheric cold plasma. The radiation impedance is weak for FM and A emissions (and extraordinaly weak for SE)

$$Z_A \approx (2V_A/c^2)\ln(2e^{\gamma-1}\Omega_i L/v_{orb}), \tag{14a}$$

$$Z_{FM} \propto 1/\omega_{pe}\omega_{pi} \tag{14b}$$

where $V_A$ is the Alfven velocity, $\gamma$ the Euler constant and $\omega_{pe}(\omega_{pi})$ the electron (ion) plasma frequency [20].

On the other hand, switching the cathodic contactor *on* from the *off* (floating) condition of section 4 would produce a

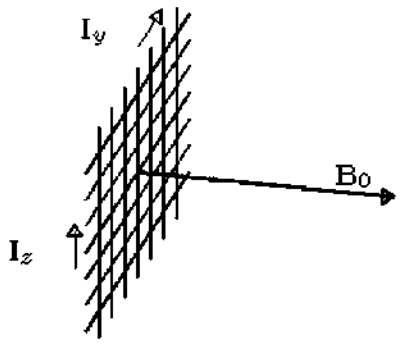


**Figure 4.** Tether array to excite whistlers.

large surge in both current and radiated power, accompanied by bias/current pulses along the tether that can be modeled as a transmission line

$$\frac{\partial I}{\partial h} = G_l \Delta V + C_l \frac{\partial \Delta V}{\partial t}, \tag{15a}$$

$$\frac{\partial \Delta V}{\partial h} = -E_m + \frac{Z_t}{L} I + L_l \frac{\partial I}{\partial t} \tag{15b}$$

allowing signal emission. Dropping time derivatives recovers the equations describing profiles $\Delta V(h)$, $I(h)$ along the distance $h$ from the bare-tether anodic end in figure 3. The conductance per unit length follows the OML collection law, $G_l \propto 1/\sqrt{|\Delta V|}$. Capacitance $C_l$ and inductance $L_l$ involve sheath radius and some radius characterizing current closure in the ambient plasma.

It was recently suggested that current modulation in tethers could generate nonlinear, low frequency wave structures attached to the spacecraft. A *magnetic pumping* process, through magnetic oscillations in the near field of the radiated wave, would result in a parametric instability. Whistlers could be excited by a planar array of electrodynamic tethers, made of two perpendicular rows of tethers that carry equal time-modulated currents with a 90° phase shift [21]. The array would fly in the orbital equatorial plane, and would be stabilized by the gravity gradient, which is perpendicular to the geomagnetic field when ignoring its tilt. Pumping by the whistler wave radiated along the field gives rise to coupled whistler perturbations with growth rate maxima at angles 38.36° and 75.93° away from it (figure 4).

Pumping fast magnetosonic waves would involve a cylindrical array of parallel tethers flying vertical in the equatorial plane. A following nonlinear stage in the wavefront moving with the orbiting array might be represented by an equation of Korteweg de Vries type, and serve to study wave interactions in space plasmas.

## 6. Radiation belt modifications

There is recent interest in artificially modifying the high-energy particle populations trapped in the Earth radiation belts. Their densities are small (typically $10\,\mathrm{m}^{-3}$) and natural replenishment rates are slow enough that mechanisms to scatter particles into their loss cone, over significant space volumes, might require reasonable power. Actually, calculations of electron loss rates due to several natural mechanisms (Whistler waves or Coulomb scattering), and due to a few high power VLF ground antennas suggest that man-made wave injections can be a dominant depletion channel. Recent observational confirmation was obtained by the Demeter satellite, which measured energetic populations at 720 km altitude. Using ground stations for intentional Belt clean-up is inefficient, however, because only a fraction of order of 1% of kilohertz power is coupled to whistler radiation through 'plasma ducts' in the ionosphere. On the other hand, *in situ* emission by an orbiting spacecraft carrying a very long antenna might be practical; the USAF DSX spacecraft will test this idea in 2010 [22].

Weak wave fields need act repeatedly over a particle to significantly modify its motion. This implies a resonance condition, which, for electrons, corresponds to the Whistler dispersion branch, with frequencies approaching values between $\sqrt{\Omega_e \Omega_i}$ (lower hybrid frequency) and $\Omega_e$, at wavelengths smaller than the skin depth $c/\omega_{pe}$,

$$1 \ll (2\pi)^2 < c^2 k^2 / \omega_{pe}^2.$$

The group velocity is nearly parallel to the magnetic field for waves that are nearly but not quite perpendicular,

$$\sqrt{m_e/m_i} \ll \omega/\Omega_e \approx k_{par}/k \ll 1. \tag{16}$$

Wavelengths range from fraction of kilometer to several kilometers, impractical for a rigid boom but possible with a flexible tether. The index of refraction $n$ is high,

$$\frac{1}{n} = \frac{\Omega_e}{\omega_{pe}} \frac{\omega}{\Omega_e} \frac{\omega_{pe}}{ck} \ll 1, \tag{17}$$

making relativistic particles interact dominantly with the magnetic field of the wave. This results in just deflections with no energy change, thus describing a pitch-angle random walk that gradually diffuses particles towards the loss-cone boundary.

A second concept would use a pair of conductive bare tethers biased at potentials of the order of 1 MV with respect to each other [23]. Since the ion current to the negative tether must equal the electron current collected by the positive tether, this one plays the role of the 3% segment in the electrically floating condition. The negative tether bias relative to the ambient plasma will then be close to the full megavolt value. Its sheath radius would both be a fraction of a kilometer and depend only weakly on the tether radius $R \ll \lambda_D$ [11],

$$1.53[1 - 2.56(\lambda_D/r_{sh})^{4/5}](r_{sh}/\lambda_D)^{4/3} \ln(r_{sh}/R) \approx e\Delta V/kT. \tag{18}$$

A fraction of all high-energy electrons and ions passing through the sheath would be scattered into their respective loss cones, while the wire radius, if small enough, could make both collected ion current and required power very small, too.

## 7. Bare tethers at Jupiter

Because of both rapid rotation (about 10 h period) and low mean density ($1.32\,\mathrm{g\,cm}^{-3}$), the stationary orbit in Jupiter,

which lies at radius

$$a_s \propto R_J \left(\rho_J/\Omega_J^2\right)^{1/3} \tag{19}$$

is one third the relative distance for Earth, or $a_s = 2.24R_J$. In turn, $B_0$ at its surface is greater than at Earth's by one order of magnitude (with the motional field near Jupiter more than one order of magnitude greater). As a result, there is magnetospheric plasma co-rotating beyond $a_s$, allowing for Lorentz thrust on tethers in prograde Jovian orbit beyond $a_s$. Also, maximum $N_0$ is typically $10^2$ times smaller than at the F-layer daytime maximum, and the Alfven velocity, $V_A \propto B_0/\sqrt{N_0}$, may be up to $10^3$ times greater than in LEO. This makes impedances for fast magneotosonic and Alfven radiations greater for Jupiter by 2 and up to 3 orders of magnitude in (14*a*) and (14*b*), both affecting the tether-current circuit and making significant signals possible [24].

Insertion in orbit and touring the Jovian moons afterwards, which are transport applications of interest, prove possible, a tens of kilometers long tape with mass a sensible fraction of the full spacecraft mass being required. Radiation dose accumulated at repeated passes through the Jovian radiation belts appears as the limiting factor for such missions. This makes missions that avoid the belts, such as NASA's Juno mission, particularly interesting. Typical power needs may be generated with tethers of moderate size and little effect on orbital dynamics because of the giant gravitational well of Jupiter [25].

This would also apply to a mission final stage, with a spacecraft starting in circular, equatorial orbit, safe below the Radiation Belts, at radius $1.3/1.4R_J$. A light, few kilometers long, thin tape bare-tether could make the spacecraft spiral in a controlled manner, over several months, while generating power onboard. A number of scientific goals might be attained. From its slowly decaying orbit the spacecraft could carry out spatially resolved observations as required for understanding transport in the atmosphere, and broad studies on its variability over different time scales. The proximity to Jupiter would allow highly accurate determination of magnetic and gravity fields and water content [26].

The initial location would be at the inner region of the *Halo* ring and the 2 : 1 Lorentz resonance, allowing for *in situ* measurements on charged grains. Lorentz resonances occur at circular equatorial orbits commensurate with periodicities of the magnetic field, $\boldsymbol{B} \approx \nabla\Psi$,

$$\Psi = -R\sum_{l=1}^{\infty}(R/r)^{l+1}\sum_{k=0}^{l}P_l^k(\cos\theta)[g_l^k\cos k\phi + h_l^k\sin k\phi] \tag{20}$$

with $g$ and $h$ Schmidt coefficients determined from observations and $P_l^k$ Schmidt-normalized associate Legendre functions. The 2-1 Lorentz resonance is the strongest one and arises from the $g_2^2$ term, which is about 0.4–0.5 G in inner magnetosphere models.

The gravity-gradient force is characteristically weak at Jupiter because of both low density and orbit radius well above $R_J$ in most missions. The tether is kept taut by a spin in the orbital plane. With the gravity-gradient torque averaging to zero, the average Lorentz torque must vanish too. Keeping a hollow cathode at just one end, end masses appropriately different make the torque vanish over the active HC spin half-period. Over the other half-period the tether is electrically floating. The emitted e-beam could result in multiple magnetic mirroring in the field of equation (20), before eventually excite auroral emissions, throughout the spacecraft orbital decay.

## 8. Electric sails in interplanetary space

Hans Alfven first considered bare wires for interplanetary transportation but the solar-wind motional field, assumed to power an electric thruster, is so weak that superconductors were required [27]. Actually, using the Lorentz force on the bare *tether* would be more efficient. Recently, an array of very thin ($R \sim 10\,\mu$m) bare tethers was proposed as a new type of solar sail, using the dynamic pressure of the solar wind for propulsion [28]. Because the sheath of each tether will be much larger than its radius, electric solar sailing may be efficient; the tether array, constituting a *virtual sail*, could be comparatively light. The Coulomb thrust is here dominant against the Lorentz thrust because of extreme values $B_{Sw} \sim 0.000\,03$ G, $v_{Sw} \sim 400\,\mathrm{km\,s^{-1}}$ and $\lambda_D \sim 10$ m, at 1 AU, say.

Early estimates of Coulomb drag on LEO satellites involved a high ion Mach number $M$, complicated 3D geometries with *radius* $R \gg \lambda_D$ and a *floating probe* condition ($-e\Delta V$ a few times $kT$). In Middle Earth Orbit, satellites such as LAGEOS I and II can float positive because of dominant photoelectron emission; tin/copper (few cm long) 'dipoles' in orbit since the 1960s involve 2D geometries, such as tethers. Coulomb forces have lately acquired relevance in *Formation-flying* satellites and in *Dusty plasmas*, where drag on charged (3D) grains involves a range of $R/\lambda_D$ and $M$ values.

Since the motional field is negligible for the e-sail, bias from a power supply will be uniform throughout the wire. The Coulomb force is thrust because the solar wind overtakes the sail, whether wire bias is positive or negative. Collecting electrons at positive bias is simpler because it requires ejecting electrons at a plasma contactor past the power supply. For a single wire, the Coulomb-to-Lorentz thrust ratio can be estimated as

$$\frac{F_{\mathrm{Coulomb}}}{F_{\mathrm{Lorentz}}} \sim \frac{2r_{sh}L \times N_0 v_{Sw}^2 m_i}{LB_0 \times 2RLeN_0\sqrt{2e\Delta V/m_e}} = \frac{v_{Sw}}{L\Omega_i}\frac{r_{sh}}{R}\sqrt{\frac{m_i v_{Sw}^2/2}{e\Delta V}}\sqrt{\frac{m_e}{m_i}}, \tag{21}$$

where a very large $r_{sh}/R$ is given in equation (18) in terms of $R/\lambda_D$ and $e\Delta V/kT$. Note the ordering $e\Delta V \sim 10\,\mathrm{keV} \gg 1/2\,m_i v_{Sw}^2 \sim 1\,\mathrm{keV} \gg kT \sim 6\,\mathrm{eV}$. A negatively biased, ion-attracting wire requires an ion gun but its Coulomb-to-Lorentz thrust ratio is larger by a factor $\sqrt{m_i/m_e} \sim 43$.

The ratio of $L\Omega_i$ to a relative velocity of interest also appears in comparing the Lorentz force $LB_0 I_{av}^{OML}$ on a drag tether in LEO with the standard aerodynamic drag by hypothetical neutrals, having the ion mass and density, on a

body of equal front-area $2RL$,

$$\frac{F_{\text{Lorentz}}}{F_{\text{neutrals}}} = \frac{I_{\text{av}}^{\text{OML}} L B_0}{2RLc_{\text{D}} m_{\text{i}} N_0 v_{\text{orb}}^2/2} \equiv \frac{4\sqrt{2}}{5c_{\text{D}}} \sqrt{\frac{m_{\text{i}}}{m_{\text{e}}}} \left(\frac{\Omega_{\text{i}} L}{v_{\text{orb}}}\right)^{3/2}, \tag{22}$$

with $c_{\text{D}}$ about 2 and the average current being 2/5 of the value in equation (7). The ratio above is usually extremely large. For oxygen ($\sqrt{m_{\text{i}}/m_{\text{e}}} \approx 171$), $L = 10\,\text{km}$, and typical LEO values (ion-gyrofrequency $\Omega_{\text{i}} \sim 200\,\text{s}^{-1}$, $v_{\text{orb}} \sim 7.5\,\text{km}\,\text{s}^{-1}$), the ratio is of order of $10^6$. This means that Lorentz drag from weakly ionized plasma can be effective where neutrals' drag is negligible.

## 9. Conclusions

Issues related to applications of conductive tethers away from transportation in LEO have been briefly reviewed. The validity of the 2D-OML collection regime at highly positive bias, and the *adiabatic trapping* of electrons by bare tethers orbiting in LEO were considered. Science applications of tethers such as generation of electron beams for atmospheric research, generation of nonlinear wave structures and *modification* of the radiation belts, as well as tether use at Jupiter and in the solar wind, were discussed.

## References


[1] Arnold D A 1987 *J. Astron. Sci.* **35** 3–18

[2] Grossi M D 1987 *Proc. 2nd Int. Conf. on Tethers in Space (Venice, Italy)* (Bologna: Società Italiana di Fisica) pp 3–8
Cosmo M L and Lorenzini E C 1997 *Tethers in Space Handbook* 3rd edn (Cambridge, MA: Smithsonian Astrophysical Observatory)

[3] Sanmartin J R and Lorenzini E C 2008 *J. Propulsion Power* **24** 851–4

[4] Carroll J A 1986 *Acta Astron.* **13** 165–74
Martinez-Sanchez M and Hastings D 1987 *J. Astron. Sci.* **35** 75–96

[5] Wilbur P and Laupa T 1988 *Adv. Space Res.* **8** 221–4
Wheelock A, Cooke D and Geis M 2008 AIAA paper 08-4596

[6] Laframboise J G 1997 *J. Geophys. Res.* **102** 2417–32
Vannaroni G, Dobrowolny M, Lebreton J P, Melchioni E, De Venuto F, Harvey C C, Iess L, Guidoni U, Bonifazi C and Mariani F 1998 *Geophys. Res. Lett.* **25** 749–52
Cooke D L and Katz I 1998 *Geophys. Res. Lett.* **25** 753–6

[7] McCoy J E *et al* 1995 *Proc. 4th Int. Conf. on Tethers in Space* vol I (Washington, DC: Smithsonian Institution) pp 57–82

[8] Sanmartin J R, Martinez-Sanchez M and Ahedo E 1993 *J. Propulsion Power* **9** 353–60

[9] Laframboise J G and Parker L W 1973 *Phys. Fluids* **16** 629–36

[10] Sanmartin J R and Estes R D 1999 *Phys. Plasmas* **6** 395–405
Estes R D and Sanmartin J R 2000 *Phys. Plasmas* **7** 4320–5
Sanmartin J R 2002 *Space Technology Course. Space Environment: Prevention of Risks Related to Spacecraft Charging, Toulouse, France* ed J P Catani and M Romero CNES/ONERA pp 515–33

[11] Sanmartin J R, Choinière E, Gilchrist B E, Ferry J-B and Martínez-Sánchez M 2008 *IEEE Trans. Plasma Sci.* **36** 2851–8

[12] Ferry J B and Martinez-Sanchez M 2003 AIAA Paper 03-4948
Choinière E and Gilchrist B 2007 *IEEE Trans. Plasma Sci.* **35** 7–22

[13] Sanmartin J R and Estes R D 2001 *Phys. Plasmas* **8** 4234–9

[14] Parker L W and Murphy B L 1967 *J. Geophys. Res.* **72** 1631

[15] Khazanov G V, Stone N H, Krivorutsky E N and Gamayunov K V 2001 *J. Geophys. Res.* **106** 10,565–79
Sanmartin J R and Estes R D 2002 *J. Geophys. Res.* **107** A11
Sanmartin J R and Estes R D 2002 *J. Geophys. Res.* **107** 1335

[16] Gurevich A V 1968 *Sov. Phys.—JETP* **26** 575
Onishi T, Martinez-Sanchez M, Cooke D L and Sanmartin J R 2001 *27th Int. Electric Propulsion Conf.* (Pasadena, CA: NASA) paper 01-245
Deux J-M 2004 Kinetic modeling of electrodynamic space tethers *MS Thesis* Department of Aeronautics and Astronautics, MIT, Cambridge, MA

[17] Bering E A, Koontz S, Katz I, Gardner B, Evans D and Ferguson D 2002 AIAA paper 02-0935
Fujii H A *et al* 2009 *Acta Astron.* **64** 313–24
Amatucci B *et al* 2009 *CE2: A CubeSat Electron Collection Experiment* (Savannah, GA: American Astronautical Society) paper AAS 09-239

[18] Martinez-Sanchez M and Sanmartin J R 1997 *J. Geophys. Res.* **102** 27,257–63
Sanmartin J R, Charro M, Pelaez J, Tinao I, Elaskar S, Hilgers A and Martinez-Sanchez M 2006 *J. Geophys. Res.* **111** A11310

[19] Winckler J R 1992 *Rev. Mod. Phys.* **64** 859–71
Strangeway R J 1980 *J. Plasma Phys.* **24** 193–212
Mishin E V and Khazanov G V 2006 *Geophys. Res. Lett.* **33** L15105

[20] Drell S D, Foley H M and Ruderman M A 1965 *J. Geophys. Res.* **70** 3131
Barnett A and Olbert S 1986 *J. Geophys. Res.* **91** 10117
Estes R D 1988 *J. Geophys. Res.* **93** 945
Sanmartin J R and Martinez-Sanchez 1995 *J. Geophys. Res.* **100** 1677

[21] Sanchez-Arriaga G and Sanmartin J R 2009 Magnetic pumping of whistler waves by tether current modulation *J. Geophys. Res.* at press

[22] Inan U S, Bell T F and Bortnik J 2002 *J. Geophys. Res.* **108** 1186–97
Abel R and Thorpe R M 1998 *J. Geophys. Res.* **103** 2385–96
Albert J M 2003 *J. Geophys. Res.* **108** 1249
Sauvaud J-A, Maggiolo R, Jacquey C, Parrot M, Berthelier J-J, Gamble R J and Rodger C J 2008 *Geophys. Res. Let.* **35** L09101

[23] Danilov V V, Elgin B A, Grafodatsky O S and Mirnov V V 2000 6th *Spacecraft Charging Technology Conf., Huntsville, AL* AFRL-VS-TR-20001578, pp 165–8
Hoyt R P and Minor B M 2005 Remediation of radiation belts using electrostatic tether structures *IEEE Aerospace Conf., Big Sky, MT* pp 583–94 doi:10.1109/AERO.2005.1559348
Zeineh C 2005 *MS Thesis* Department of Aeronautics and Astronautics, MIT, Cambridge, MA

[24] Sanchez-Torres A, Sanmartin J R, Donoso J M and Charro M 2009 The radiation impedance of electrodynamic tethers in polar Jovian orbit *Adv. Space Res.* submitted

[25] Sanmartin J R, Charro M, Lorenzini E C, Garret H B, Bombardelli C and Bramanti C 2008 *IEEE Trans. Plasma Sci.* **36** 2450–8
Sanmartin J R, Charro M, Lorenzini E C, Garret H B, Bombardelli C and Bramanti C 2009 *IEEE Trans. Plasma Sci.* **37** 620–6
Bombardelli C, Lorenzini E C and Sanmartin J R 2009 *J. Propulsion Power* **25** 415–23

[26] Sanmartin J R, Bombardelli C, Charro M and Lorenzini E 2009 AIAA paper 09-4549

[27] Alfven H 1972 *Science* **176** 167–8

[28] Janhunen P 2004 *J. Propusion Power* **20** 763–4
Janhunen P 2009 *Ann. Geophys.* **27** 1439–47